Tenth International Conference on Computational Fluid Dynamics (ICCFD10), Barcelona,Spain, July 9-13, 2018

ICCFD10-2018-xxxx

Large eddy simulation for automotive aerodynamics with Alya

Oriol Lehmkuhl *, Georgios Chrysokentis*, Samuel Gomez* and Herbert Owen*
Corresponding author: herbert.owen@bsc.es

* Barcelona Supercomputing Center (BSC).

Abstract

The prodigious potential offered by the ever-growing computing infrastructure is fostering the use of large eddy simulation for automotive aerodynamics. This approach, which resolves the larger dynamically important eddies and models only the smaller ones, provides significant improvement over RANS when there are important separated regions or transient phenomena such as noise generation.

In the search for high fidelity LES solution Alya has recently undergone a significant transformation departing from the use of the Variational Multiscale approach and implicit temporal discretization. Nowadays, Alya has switched to an explicit temporal discretization, without any stabilization other than the pressure stabilization introduced by the fractional step scheme. When using a energy conserving discretization for the convective term together with an explicit turbulent model, numerical stabilization of the convective term in the Navier Stokes equations is not needed. The Vreman turbulence model is used in this work. For the simulation of high Reynolds number turbulent flows, such as those encountered in automotive applications, the use of wall modeling is mandatory with current computational resources. Significant improvements in the implementation of wall modeling for finite element methods proposed recently are tested in this work for highly complex geometries. Comparison of the numerical results for both the Ahmed and DrivAer bodies against experimental results from the literature shows that Alya can provide very accurate results.

1 Introduction

Due to legislation to reduce the emission of greenhouse effect gases, the automotive industry has been forced to decrease the energy consumption of their vehicles. As a consequence, it makes a lot of sense to increase the effort to reduce fuel consumption by diminishing the aerodynamic drag forces which account for approximately 60% of the fuel consumption under normal highway driving conditions. Moreover, for electric vehicles that are expected to dominate the market the next decade, range is one the most important challenges. It can be improved by means of increasing the size, weight and cost of batteries or by aerodynamic drag reduction. Hence, external aerodynamic is one of the most important aspects of road vehicles design due to its impact on performance features such as dynamic behavior, noise and energy consumption.

For the improvement and optimization of the car geometry design, it is essential to comprehend the flow structures it generates. This can be done using both numerical or experimental methods. Thanks to the huge advances in computational fluids dynamics coupled to constant reduction of the cost of computational hardware, numerical methods are constantly increasing their share in the design process. However, due to the high complexity of turbulent flows around complex geometries at high Reynolds numbers, car companies still rely on blend between numerical simulations and wind tunnel data for their design process. Experimental data are constantantly used to validate and improve numerical models.

Unfortunately most of the experimental data available to the research community corresponds to simplified car models such as the Ahmed [1] and SAE [2] cars which do not capture all of the complex phenomena around real cars. Experimental data for production vehicles is usually of limited access due to its confidentiality. The DrivAer body has been developed at the Institute of Aerodynamics and Fluid Mechanics at the

Technische UniversitâĂŤt MÂÿnchen (TUM) [3, 4, 5] to close the gap between simplified and real cars. The first experimental simulations of the DrivAer body (2012) were carried out in the updated Wind Tunnel of the previously mentioned institute. Since then, different experimental and numerical simulations have been performed. On the experimental side, additional research has been accomplished at the Institute of Fluid Dynamics and Technical Acoustics at the "Technische UniversitâĂŤt Berlin"(TUB) [6, 7]. The numerical background focuses mainly on RANS and DES simulations (see Ashton et al. [8] or Guilmeneau [9, 10]). Little research has been performed using LES [11]. Our objective is to better understand the flow by means of LES and assess the performance of the HPC code Alya first for both the Ahmed and DrivAer models.

The validation starts with the Ahmed [1] car which has latter been experimentally tested by Lienhart et at. [12] with the objective to develop, refine, and validate turbulence models and is therefore perfectly suited for our objective. Moreover, taking advantage of observations made by Krajnovic et al. [13] the Reynolds number is reduced to 200000 and thus the use of wall functions is avoided. In this way, validation with the simplified geometry focuses on the LES model while the coupling between the LES model and the wall modeling is performed with the DrivAer body.

In Section 2 a brief overview of the physical and numerical model used in this work is presented. Our recent improvements to the wall modeling approach for LES are summarized in 3. The numerical results and their comparison with experimental results available in the literature, for both the simplified and realistic car bodies are presented in Sections 4 and 5. Finally, the conclusions are presented in Section 6.

2 Physical and Numerical model

Alya is a high performance computing multiphysics code developed at the Barcelona Supercomputing Center. It has been designed from scratch for massively parallel supercomputers, and it is part of the PRACE benchmark suite for Computational Fluid Dynamics. For further details on its computational capabilities and scalability results up to 100.000 processors the reader is referred to [14]. The incompressible Navier Stokes module used in this work is based on a standard Galerkin Finite Element discretization.

For LES some kind of dissipation must be introduced to take into account the effect of the subgrid scales. Within the finite element community a widely accepted approach is to introduce this dissipation implicitly by means of a suitably designed numerical method [15, 16, 17]. Outside the finite element community, the most widespread approach is to resort to an explicit turbulent viscosity thus uncoupling the numerical method from the physical one. In the work we follow the latter approach which has proved to provide superior results for turbulent flows [18] even with a finite element discretization. The eddy viscosity model proposed by Vreman [19] is used.

For turbulent high Reynolds number flows a discretization of the convective term that conserves kinetic energy has been widely recognized as a key ingredient for obtaining stable high accuracy solutions without artificial numerical dissipation [20, 21, 22, 23]. In the LES context numerical dissipation can alter the energy cascade, and thus the transfer of energy to the small scales. As initially proposed by Verstappen and Veldman [22], the key idea of the method we use is that the discrete problem mimics the fundamental properties of the continuous Navier Stokes equations: the convective operator is approximated by a skew-symmetric operator that conserves energy, the pressure gradient operator is equal to the transpose of the divergence operator and, the diffusive operator is approximated by a symmetric, positive-definite matrix. In the finite volume context the method has been extended to unstructured collocated grids in [24, 23]. In the finite element context an equivalent scheme is recovered when standard Galerkin discretization (without any added stabilization) is used; together with an energy conserving discretization for the convective term and linear equal order interpolation for velocity and pressure. Since this interpolation does not satisfy the inf-sup condition, a fractional step scheme[25, 26] is used to introduce the required pressure stabilization [27]. It does not depend on user defined parameters and introduces a kinetic energy dissipation of $\mathcal{O}\left(\delta t * h^{p+1}\right)$ where δt is the time step size, h is the mesh size and p is the order of finite element functions [18]. For linear elements the dissipation is of $\mathcal{O}\left(\delta t * h^2\right)$, as in the unstructured collocated finite volume scheme [24, 23], while higher order spatial interpolations lead to reduced dissipation. Two key features of the proposed numerical formulation are the avoidance of user defined parameters and its simplicity since only Galerkin terms are used. In the present work only linear elements have been used due to meshing limitations but very promising results have already been obtained for simple geometries with quadratic elements [18].

For the discretization of the convective term the EMA scheme recently proposed in [28] is used. This work also includes a complete review of the different discretizations for the convective term within the FE context and their conservation properties. The EMA scheme not only conserves kinetic energy but also momentum and angular momentum. In our experience, it provides better results than the skew-symmetric form which only conserves kinetic energy.

A Runge-Kutta explicit temporal discretization is used for both convective and diffusive terms. For the examples presented in this work, a third order version is used since it has proven to provide the best balance between accuracy and computation cost for time step sizes used in this work, which must accurately resolve the temporal scales present in the flow. This explicit temporal discretization introduces a kinetic energy dissipation of $\mathcal{O}\left(\delta t^3\right)$. Alternative Runge-Kutta schemes with lower dissipation have been proposed in [29] which introduce noticeable improvement in other cases but not in those presented in this paper. In order to reduce the computational cost, we have used the approximate projection method proposed in [30]. It allows to solve the linear system for the pressure only once per time step instead of once per Runge-Kutta substep. In the examples presented in this work, no degradation of the the results has been observed due to its use. An eigenvalue-based time-step estimator [31] is used to adaptively determine the time step size.

3 Wall modeling

In order to deal with high Reynolds numbers typical of real automotive applications, the use of wall modeling is mandatory. The size of the dynamically important vortices at high Reynolds numbers becomes too small close to the wall to be resolved even with the most powerful available supercomputers available nowadays or those foreseeable in the close future. Therefore, the inner part of the boundary layer needs to be modeled. Wall modeling for large eddy simulation is an active area of research and the reader is referred to [32, 33, 34, 35] for additional information on the subject and estimations of the cost of wall resolved simulations.

The classical finite element approach for wall modeling [36] supposes that there exists a very thin region close to the wall that is not actually included in the mesh as shown in Figure 1. That is, the mesh starts at a distance, d, from the wall. In this region the flow is modeled using Reichardt's extended law of the wall [37]. The normal component of the velocity at point A is prescribed prescribed to zero. The tangential velocity modulus and the distance to wall, d, are used to calculate a tangential traction that is applied in the opposite direction to the velocity. According to the classification presented in a recent review by Larsson et al. [34] the classical approach used by the finite element community can be classified as a hybrid LES/RANS model, since the LES is not actually extending all the way to the real wall. Instead in classical finite volume and finite difference implementations the LES mesh extends all the way to the wall and can thus be classified as a wall-stress model. We have recently discovered that the classical finite element approach for implementing the wall law for LES provides quite poor results [38].

In the search for better wall modeling approaches for finite element LES, the work by Kawai and Larsson [39], has recently been adapted to finite elements with spectacular results. For a channel flow at $Re_\tau = 2000$ on a 64^3 grid, switching from the classical finite element approach to the approach proposed in [39], the error in the mean velocity was reduced by nearly an order of magnitude [38]. The key difference in the new approach is that the mesh extends all the way to the wall and the velocity used to obtain the traction to be applied at the wall (point B in Figure 1) is that of some point (point D in Figure 1) at a user defined distance from the wall in the normal direction. When this distance is chosen as the normal size the first element, a method that is equivalent to the classical implementation used by the finite difference community is recovered. Cabot and Moin [40] explain that part of the wall modeling errors are due to subgrid modeling inaccuracies in the first few off-wall nodes as a result of the wall proximity. Based on this observation, Kawai and Larsson [39] have proposed that better results, including a reduction in the logarithmic layer mismatch, can be obtained by using the velocity at a point further away from the wall to calculate the traction to be applied at the wall. From the previous observations , the usage of the velocity at point A (Figure 1), as in done in the classical finite element approach, seems to be the worse option. The results in [38] show that, as suggested in [39], using the velocity at a point further towards the interior of the domain (point D in Figure 1) instead of the velocity at the first node from the wall (point C in Figure 1) helps to improve the solution. Moreover, it is shown that either of those two solutions is much better than the one obtained with the classical finite element approach.

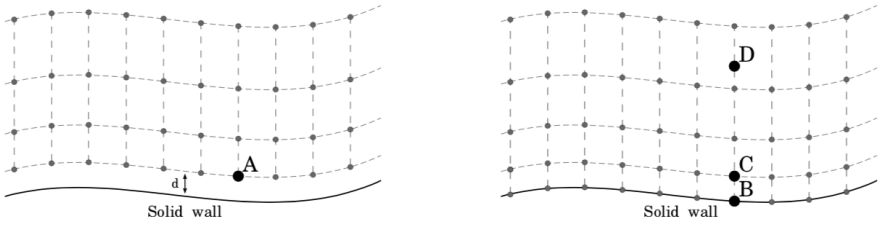

Figure 1: Standard finite element wall modeling approach (left) and improved alternative (right)

In [34] it is suggested that the velocity used to calculate the traction at the wall is obtained at a distance corresponding to 20 percent of the boundary layer height. From the visual observation of preliminary simulations we have chosen this distance as 4 times the height of the first element. In a recent publication [41], it is mentioned that one of the biggest drawbacks of the formulation proposed by Kawai and Larsson [39] is that the the method is not well suited for complex geometries and an alternative method is proposed. We are not in the position to suggest which approach is better, but we believe that the wall modeled numerical examples presented in this work show that significant geometrical complexity can be handled. In order to do so, a solution must be adopted for small gaps. In such cases, the point where the velocity is obtained (point D in Figure 1) might fall outside the fluid domain. For such points, the approach we have followed is to reduce the distance by half iteratively until the point falls inside the domain. Those points are typically found in regions where the validity of the wall law is debatable anyway. Moreover, in the worse case scenario, something similar to the classical finite difference/volume approach is recovered for those points while the rest benefit from the improved treatment. The wall modeled results in this work are possibly the most geometrically complex examples of the application of the method suggested by Kawai and Larsson [39].

4 Ahmed car

The Ahmed car is probably the most well known simplified car model used for vehicle aerodynamics. The front part has a rounded shape and at the rear the top ends at a slant angle. Ahmed proposed the shape and experimentally studied the effect of the slant angle. Despite the simplified geometry, it exhibits most of the flow features encountered in rear part of real cars such as the large recirculation zone and a complex vortex interaction of the flow coming from the slant side edges. It was observed that most of the drag is produced at the rear end and that its behaviour changes significantly at a slant angle of 30 degrees which corresponds to the maximum drag. Above this angle, the drag coefficient falls significantly due to a an important change in the flow pattern characterized by weaker lateral counter rotating vortices, separation along all of the top edge and no flow reattachment. For slant angles smaller than 30 degrees, the flow separates only in the center of the top edge and the much stronger counter-rotating vortices induce the flow to reattach at the slanted surface.

Lienhart et at. [12] experimentally tested the model using laser doppler anemometry for two slant angles at five degrees to each side of the critical value with the objective to develop, refine, and validate turbulence models. While the 35 degree has proved to be easy to reproduce correctly with RANS turbulence, the complex flow pattern behind the car at a 25 degree slant angle has not been simulated satisfactorily with RANS turbulence models. The latter has thus become the most chosen case for LES and DES simulations. Despite the the simplicity of the geometry compared to a real car, the case has not been simple to simulate even with such approaches .

Based on the previous observations, in this work a 25 degree slant angle is simulated using LES. Taking advantage of the conclusions from [13] that show that the flow is insensitive to the Reynolds number between $Re = 2.0 \cdot 10^5$ and $Re = 7.68 \cdot 10^5$, simulations are performed at the lower value so that this case is used to validate the LES implementation while wall modeling is tested in the DrivAer example. An unstructured mesh with 14M tetrahedral and prism elements and 5.6M nodes is used. The mesh has been refined close to the body and mainly in the recirculation region formed behind the car as can be seen in Figure 2. The time

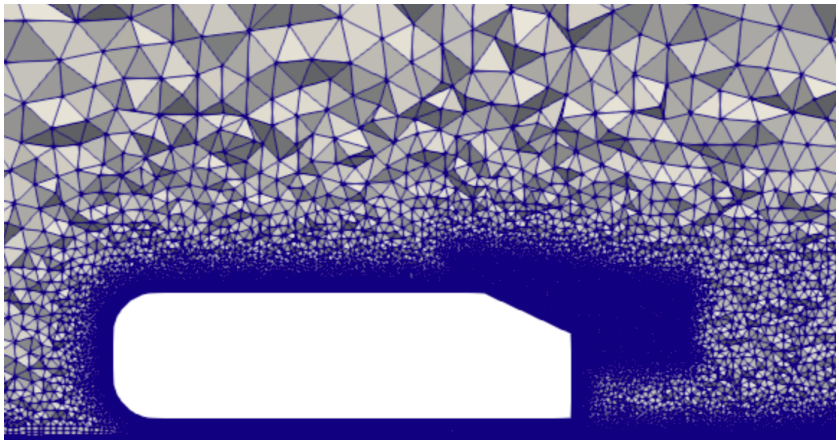

Figure 2: Mesh for the Ahmed body

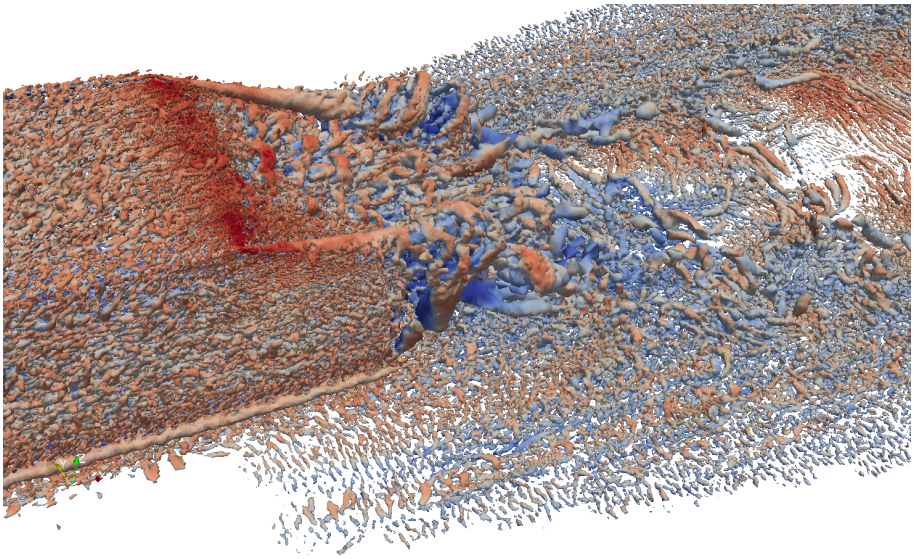

Figure 3: Q criterion of the instantaneous vorticity showing the mains flow structures

step has been chosen adaptively setting a CFL value of 0.5 according to the method mentioned in Section 2. A total of 10 time units have been run and the average results correspond to the last 3 time units.

The isosurface for the Q criterion of the vorticity (Figure 3) allows to visualize most of the flow structures occurring behind the body. Several horseshoe vortex can be observed on the upper region of the rear slant surface together one corner vortex on each side.

A pressure drag of 0.234 and a total drag of 0.285 are obtained numerically. These results match the experimental results [1] much better than those obtained in [42, 43, 44].

5 DrivAer

The second case is a realistic generic car model called the DrivAer body that has become widely accepted within the aerodynamics community. The model has been developed at TUM, where it has been experimen-

tally tested using a 40% scaled model [3, 4, 5, 45] at $Re = 4.87 \cdot 10^6$. In the Munich wind tunnel, cases with and without moving ground have been simulated taking advantage of the belted wind tunnel. There exist some small discrepancies between the values presented in the different works. To exemplify the differences we shall concentrate in the Fastback model with Smooth underbody, Mirrors and Wheels (F_S_wM_wW). Experimental results with and without ground simulation are presented in Table 1 and 2 respectively. For the case with ground simulation, there is a difference of 0.022 between the maximum and minimum values for the drag coefficient while the first author is the the same for both works. Only one lift value is available. Moreover, the wheels that have been used do not match those of the DrivAer model. Instead generic wheels with a slightly different shape, diameter and width have been used [45]. For the case without ground simulation a 25% scaled model at Re from $0.75 \cdot 10^6$ to $2.8 \cdot 10^6$ has been tested at the a wind tunnel in Berlin [6, 7]. Despite the Reynolds number is lower, in [6] a nearly independent behavior of the drag coefficient for Reynolds numbers above $Re = 2.25 \cdot 10^6$is observed. Their results are also included in Table 2. The drag coefficient differs up to 0.012 even for cases tested in the same wind tunnel. For the case without ground simulation three different lift values are provided, the maximum difference is 0.153 and corresponds to two test performed at the wind tunnel in Berlin [6, 7]. The second publication [7] does not even mention the difference with the previous one. Comparing with the results from [5] does not allow to make a clear choice either. Therefore the main conclusion is that there is some spread in the drag coefficient that could provide some idea of the accuracy of the measurement. For the lift coefficient the spread is so big that is quite difficult to say which might be the correct result.

In [3, 4, 45] there is no specification of the position of the wheel relative to the ground but we suppose it is in contact with it, at least for the cases involving moving ground. For the numerical modeling this introduces significant difficulties in generating the mesh. In [6] it is specified that there exists a gap between the ground and the wheel of 1.5 mm and that the distance between the center of the wheel and ground is 83 mm. Since the radius of the DrivAer wheel model scaled to 25% is 79.625 mm it seems that some generic wheel must have been used. In [7] the gap between the wheel and the ground is also 1.5 mm but there is no information about the wheel diameter. We would like to think that the correct wheel has been used in [7] and that this explains the differences in drag coefficient with [6] . It is hard to believe that it could explain the differences in lift coefficient. Numerical results have been obtained using an IDDES approach in [46, 47] for the fastback geometry.

	w/o GS		w GS	
	C_D	C_L	C_D	C_L
Numerical	0.262	-0.111	0.265	-0.022
Heft [5]	0.261	0.01	0.265	-0.06
Heft [3]	0.254	n/a	0.243	n/a
Heft [4]	n/a	n/a	0.241	n/a
Wieser [7]	0.258	-0.096	n/a	n/a
Strangfeld [6]	0.249	0.057	n/a	n/a
Mack [45]	0.249	n/a	0.247	n/a

Table 1: C_D and C_L Fastback configuration

Refinement Zones	Max Surface Length mm	Max Volume Length mm
Green	10	20
Red	20	40
Blue	40	80

Table 2: Maximum element size for each refinement zone

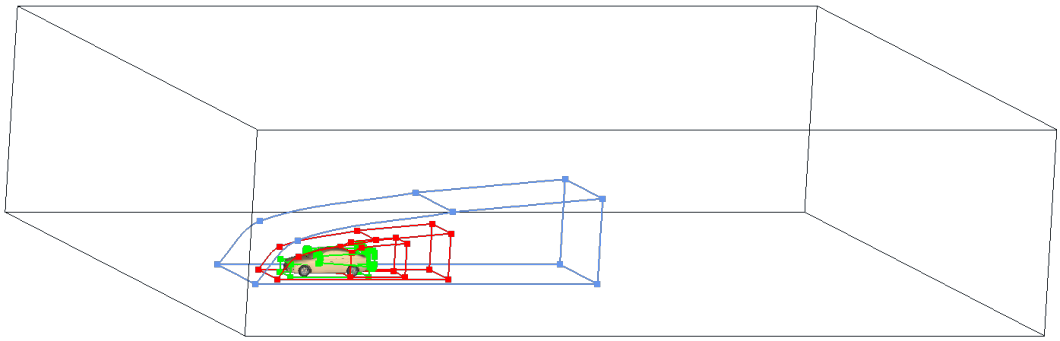

Figure 4: Computational domain and different refinement zones

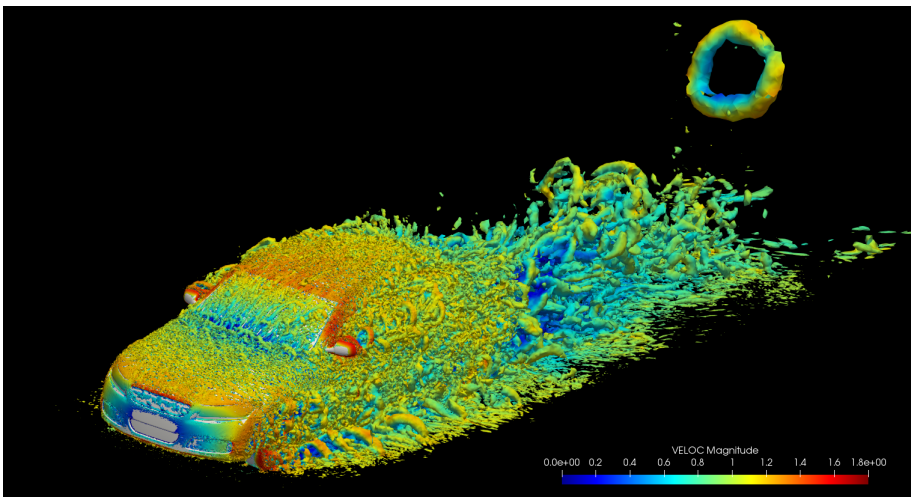

Figure 5: Q criterion for the vorticity colored by the velocity magnitude for the Drivaer with rotating wheels

The computational domain has a length of 10L, a height of 8H and a width of 11W, where the vehicle is situated at 2L from the inlet boundary at the symmetry plane as shown in Figure 4. The Figure also includes a detail of the refinement zones. The sizes used in the different zones are presented in Table 2.

In this work, the fastback geometry with smooth underbody, mirrors and both moving and fixed ground is simulated. The Reynolds number with respect to the vehicle length is $Re = 4.87 \cdot 10^6$ which requires the use of wall modeled LES. In Figure 5 the Q criterion for the vorticity colored by the velocity magnitude for the fastback case with rotating wheels is presented. For this case the drag coefficient, $C_d = 0.265$, and the lift coefficient, $C_l = -0.022$, are in good agreement with experimental results [5].

Figure 6 combines the pressure coefficient over the car body with the streamlines for the mean flow for the fastback DrivAer model in the case without moving ground so that the results are comparable with those from [6]. The flow pattern in the symmetry plane compares well with the experimental results from [6]. Instead there is some deviation for the pressure coefficient. However, there seem to be some inconsistencies in the pressure coefficient results in [6] as can be seen by comparing their Figures 6 and 7.

Finally, the streamlines for the mean flow at the car rear are shown in Figure 7. A good match with the experimental surface visualization presented in [7] is obtained.

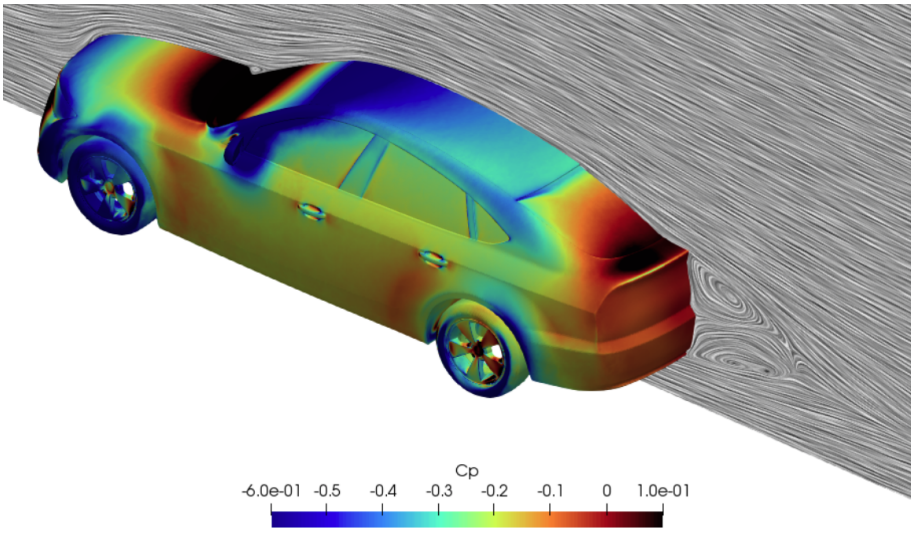

Figure 6: Pressure coefficient and line integral convolution on symmetry plane for the average flow

Figure 7: Streamlines for the average flow

6 Conclusions

The validation of the Alya code against experimental results for two car bodies shows an acceptable behaviour, but slightly different trends are observed. While the the geometry of the first case is much simpler that the first one, available numerical results from the literature show that it is actually a much harder case to predict numerically. Alya performs very well for this case. For the DrivAer benchmark, there is a smaller spread between the numerical results despite the much higher complexity of the geometry. Moreover the spread in the numerical results is comparable with the spread of the experimental results. While the experimental results from [12] have been performed with the specific objective to develop, refine, and validate turbulence models, the objective of the experimental results for the DrivAer body seem to be more general.

Acknowledgements

This work has been partially supported by the Energy oriented Centre of Excellence (EoCoE) (Grant Agreement number 676629, funded within the H2020 framework of the European Union). Georgios Chrysokentis is grateful to a doctoral grant by the Spanish Ministry of Economy, Industry and Competitiveness with grant number BES-2013-066343.

References

[1] SR. Ahmed, G. Ramm, and G. Faltin. Some salient features of the time averaged ground vehicle wake. *SAE Technical Paper 840300*, 1984.

[2] A. Cogotti. Parametric study on the ground effect of a simplified car model. *SAE Technical Paper 980031*, 1998.

[3] Angelina I. Heft, Thomas Indinger, and Nikolaus A. Adams. Experimental and numerical investigation of the drivaer model. *ASME*, 2012.

[4] Angelina I. Heft, Thomas Indinger, and Nikolaus A. Adams. Introduction of a new realistic generic car model for aerodynamic investigations. *SAE*, 2012.

[5] Angelina I. Heft. *Aerodynamic Investigation of the Cooling Requirements of Electric Vehicles*. PhD thesis, Technische Universitat Munchen, 2014.

[6] Christoph Strangfeld, Dirk Wieser, Hanns-Joachim Schmidt, Rene Woszidlo, Christian Nayeri, and Christian Paschereit. Experimental study of baseline flow characteristics for the realistic car model drivaer. *SAE*, 2013.

[7] Dirk Wieser, Hanns-Joachim Schmidt, Stefan Mueller, Christoph Strangfeld, Christian Nayeri, and Christian Paschereit. Experimental comparison of the aerodynamic behavior of fastback and notchback drivaer models. *SAE*, 2014.

[8] Neil Ashton, Alaister West, Sylvain Lardeau, and Alistair Revell. Assessment of rans and des methods for realistic automotive models. *Computers and Fluids*, 2016.

[9] Emmanuel Guilmineau. Numerical simulations of ground simulation for a realistic generic car model. *ASME*, 2014.

[10] Emmanuel Guilmineau. Numerical simulations of flow around a realistic generic car model. *SAE*, 2014.

[11] David Aljure, Joan Calafell, Baez, and Asensi Oliva. Flow over a realistic car model: Wmles assessment and turbulent structures. *Conference: Direct and Large-Eddy Simulation 11*, 2017.

[12] H. Lienhart and S. Becker. Flow and turbulent structure in the wake of a simplified car model. *SAE Paper*, 2003-01-0656, 2003.

[13] S. Krajnovic and L. Davidson. Large-eddy simulation of the flow around simplified car model. *SAE Technical Paper*, 2004-01-0227, 2004.

[14] Mariano Vazquez, Guillaume Houzeaux, Seid Koric, Antoni Artigues, Jazmin Aguado-Sierra, Ruth Aris, Daniel Mira, Hadrien Calmet, Fernando Cucchietti, Herbert Owen, Ahmed Taha, Evan Dering Burness, Jose Maria Cela, and Mateo Valero. Alya: Multiphysics engineering simulation toward exascale. *Journal of Computational Science*, 14:15 – 27, 2016. The Route to Exascale: Novel Mathematical Methods, Scalable Algorithms and Computational Science Skills.

[15] Volker Gravemeier, Michael W. Gee, Martin Kronbichler, and Wolfgang A. Wall. An algebraic variational multiscale multigrid method for large eddy simulation of turbulent flow. *Computer Methods in Applied Mechanics and Engineering*, 199(13):853 – 864, 2010. Turbulence Modeling for Large Eddy Simulations.

[16] Oriol Colomes, Santiago Badia, Ramon Codina, and Javier Principe. Assessment of variational multiscale models for the large eddy simulation of turbulent incompressible flows. *Computer Methods in Applied Mechanics and Engineering*, 285:32 – 63, 2015.

[17] Ramon Codina, Javier Principe, Oriol Guasch, and Santiago Badia. Time dependent subscales in the stabilized finite element approximation of incompressible flow problems. *Computer Methods in Applied Mechanics and Engineering*, 196(21):2413 – 2430, 2007.

[18] O. Lehmkuhl, G. Houzeaux, H. Owen, G. Chrysokentis, and I. Rodriguez. A low-dissipation finite element scheme for scale resolving simulations of turbulent flows. *Journal of Computational Physics*, submitted.

[19] A. W. Vreman. The filtering analog of the variational multiscale method in large-eddy simulation. *Physics of Fluids*, 15(8):L61–L64, 2003.

[20] Akio Arakawa. Computational design for long-term numerical integration of the equations of fluid motion: Two-dimensional incompressible flow. part i. *Journal of Computational Physics*, 1(1):119 – 143, 1966.

[21] Y. Morinishi, T.S. Lund, O.V. Vasilyev, and P. Moin. Fully conservative higher order finite difference schemes for incompressible flow. *Journal of Computational Physics*, 143(1):90 – 124, 1998.

[22] R.W.C.P. Verstappen and A.E.P. Veldman. Symmetry preserving discretization of turbulent flow. *Journal of Computational Physics*, 187(1):343 – 368, 2003.

[23] Lluis Jofre, Oriol Lehmkuhl, Jordi Ventosa, F. Xavier Trias, and Assensi Oliva. Conservation properties of unstructured finite-volume mesh schemes for the Navier–Stokes equations. *Numerical Heat Transfer, Part B: Fundamentals*, 65(1):53–79, 2014.

[24] F.X. Trias, O. Lehmkuhl, A. Oliva, C.D. Perez-Segarra, and R.W.C.P. Verstappen. Symmetry preserving discretization of Navier–Stokes equations on collocated unstructured grids. *Journal of Computational Physics*, 258:246 – 267, 2014.

[25] A.J. Chorin. A numerical method for solving incompressible viscous problems. *Journal of Computational Physics*, 2:12–26, 1967.

[26] R. Temam. Sur l'approximation de la solution des équations de Navier–Stokes par la méthode des pas fractionaires (I). *Archives for Rational Mechanics and Analysis*, 32:135–153, 1969.

[27] R. Codina. Pressure stability in fractional step finite element methods for incompressible flows. *Journal of Computational Physics*, 170:112–140, 2001.

[28] Sergey Charnyi, Timo Heister, Maxim A. Olshanskii, and Leo G. Rebholz. On conservation laws of Navier-Stokes Galerkin discretizations. *Journal of Computational Physics*, 337:289 – 308, 2017.

[29] F. Capuano, G. Coppola, L. Rández, and L. de Luca. Explicit Runge-Kutta schemes for incompressible flow with improved energy-conservation properties. *Journal of Computational Physics*, 328:86 – 94, 2017.

[30] F. Capuano, G. Coppola, M. Chiatto, and L. de Luca. Approximate projection method for the incompressible Navier–Stokes equations. *AIAA Journal*, 54:2179 – 2182, 2016.

[31] F. X. Trias and O. Lehmkuhl. A self-adaptive strategy for the time integration of Navier–Stokes equations. *Numerical Heat Transfer, Part B: Fundamentals*, 60(2):116–134, 2011.

[32] Ugo Piomelli, , and Elias Balaras. Wall-layer models for large-eddy simulations. *Annual Review of Fluid Mechanics*, 34(1):349–374, 2002.

[33] Ugo Piomelli. Wall-layer models for large-eddy simulations. *Progress in Aerospace Sciences*, 44(6):437 – 446, 2008. Large Eddy Simulation - Current Capabilities and Areas of Needed Research.

[34] Johan Larsson, Soshi Kawai, Julien Bodart, and Ivan Bermejo-Moreno. Large eddy simulation with modeled wall-stress: recent progress and future directions. *Mechanical Engineering Reviews*, 3(1):15–00418–15–00418, 2016.

[35] Sanjeeb T. Bose and George Ilhwan Park. Wall-modeled large-eddy simulation for complex turbulent flows. *Annual Review of Fluid Mechanics*, 50(1):535–561, 2018.

[36] David Lacasse, Aric Turgeon, and Dominique Pelletier. On the judicious use of the k–ϵ model, wall functions and adaptivity. *International Journal of Thermal Sciences*, 43(10):925 – 938, 2004.

[37] H. Reichardt. Vollständige darstellung der turbulenten geschwindigkeitsverteilung in glatten leitungen. *Zeitschrift fuer Angewandte Mathematik und Mechanik*, 31:208–219, 1951.

[38] H. Owen, G. Chrysokentis, M. Avila, D. Mira, G. Houzeaux, J.C. Cajas, and O. Lehmkuhl. Wall-modelled large-eddy simulation in a finite element framework. *Journal of Computational Physics*, submitted.

[39] Soshi Kawai and Johan Larsson. Wall-modeling in large eddy simulation: Length scales, grid resolution, and accuracy. *Physics of Fluids*, 24(1):015105, 2012.

[40] W. Cabot and P. Moin. Approximate wall boundary conditions in the large-eddy simulation of high reynolds number flow. *Flow, Turbulence and Combustion*, 63, 2000.

[41] Xiang I. A. Yang, George Ilhwan Park, and Parviz Moin. Log-layer mismatch and modeling of the fluctuating wall stress in wall-modeled large-eddy simulations. *Phys. Rev. Fluids*, 2:104601, Oct 2017.

[42] D.E. Aljure, O. Lehmkuhl, I. RodrÃŋguez, and A. Oliva. Flow and turbulent structures around simplified car models. *Computers and Fluids*, 96:122 – 135, 2014.

[43] S. Krajnovic and L. Davidson. Flow around a simplified car: Part1: Large eddy simulation. *ASME: Journal of Fluids Engineering*, 127, 2005.

[44] Eric Serre, Matthieu Minguez, Richard Pasquetti, Emmanuel Guilmineau, Gan Bo Deng, Michael Kornhaas, Michael Schafer, Jochen Frohlich, Christof Hinterberger, and Wolfgang Rodi. On simulating the turbulent flow around the ahmed body: A french–german collaborative evaluation of les and des. *Computers & Fluids*, 78:10 – 23, 2013. LES of turbulence aeroacoustics and combustion.

[45] Steffen Mack, Thomas Indenger, and Nikolaus A. Adams. The interior design of a 40% scaled drivaer body and first experimental results. *ASME*, 2012.

[46] N. Ashton, A. West, S. Lardeau, and A. Revell. Assessment of rans and des methods for realistic automotive models. *Computers and Fluids*, 128:1 – 15, 2016.

[47] E. Guilmineau. Numerical simulations of flow around a realistic generic car model. *SAE Int. J. Passeng. Cars - Mech. Syst*, 7(2):646–653, 2014.